Journal of Modern Researches on Electronic Defense Systems

Receive: 26 Decemebr 2025 Accept:12 June 2026

A Breakthrough Approach to Multi-Threat Electronic Warfare with Deep Learning

Zohreh. Dorrani*
*Corresponding Author: zdorrani@yahoo.com

Department of Electrical Engineering, Payame Noor University, Tehran, Iran.

Abstract – *Deep learning-based anti-jam beamforming for radar and communication systems in hostile electromagnetic environments. This paper presents a one-dimensional convolutional neural network-based anti-jam beamforming technique for radar and communication systems in hostile electromagnetic environments. A one-dimensional convolutional neural network with a specially designed architecture is proposed to directly learn the nonlinear relationship between received signal features and beamforming coefficients. Therefore, the computationally intensive covariance matrix inversion of conventional adaptive techniques is avoided. A proper network architecture is designed to obtain a trade-off between the beamforming performance and the setting complexity. The resultant neural network can be implemented in real-time on the existing hardware. Simulation results demonstrate that deep nulls of greater than -60dB can be achieved for jamming directions. The desired signal is attenuated by approximately 0dB without distortion. A significant SINR improvement of approximately +9.6dB and sidelobe levels of -12dB to -15dB are obtained to suppress the effects of multiple interference sources. Comparative analysis with recently proposed state-of-the-art anti-jam techniques shows that the proposed technique achieves deeper nulls and preserves the main-lobe while obtaining desired signal gains. Further, the proposed technique is robustly tuned to account for array imperfections and angular uncertainties by incorporating a diagonal loading and due adaptive constraint. The proposed technique demonstrates robust performance against multiple jamming sources with angular uncertainties.*

Keywords: Anti-jam beamforming, Deep learning, Convolutional neural network, Adaptive radar, Electronic warfare.

1. Introduction

The emergence and evolution of deep learning [1] over the past decade has instigated a fundamental revolution in signal processing, computer vision, and wireless communications. Deep neural networks [2] have the capacity to learn hierarchical representations from complex data. As a result, they have achieved remarkable accomplishments across diverse domains, ranging from image recognition and natural language processing to time-series forecasting and dynamic system optimization. In array processing and multi-antenna systems [3], deep learning has introduced a paradigm-shifting approach that diverges from conventional analytically-driven mathematical models toward data-driven methodologies [4, 5]. This change results from the inherent capability of deep architectures to learn complex nonlinear features from multidimensional data, which is a key advantage over analytical methods in realistic environments with large uncertainties. Applications of deep learning in electrical engineering, particularly in multi-antenna signal processing [6] , have experienced exponential growth in recent years. Convolutional neural networks, initially developed for image processing, have now been adapted for extracting spatial features from array data. Recurrent networks and long short-term memory architectures are employed to model temporal dependencies in non-stationary signals [7]. Attention-based architectures and transformers have garnered significant interest in multidimensional signal processing due to their capacity to model long-term [8] dependencies and non-local relationships in complex data. These advancements have led to the development of self-adjusting systems capable of delivering optimal performance in dynamic and unpredictable environments.

In the specific context of adaptive beamforming and interference suppression, deep learning-based approaches [4, 9, 10] have opened promising research pathways. Methods employing deep neural networks [11] can learn complex nonlinear mappings between received signal features and optimal beamforming coefficients directly from data, without requiring simplifying assumptions typically necessary in analytical approaches. This capability proves particularly valuable in complex operational scenarios involving multiple interference sources, multipath channels, and non-ideal array conditions. Deep networks can discover hidden spatiotemporal patterns in received data and infer optimal adaptation strategies that remain effective even in the presence of unknown or incomplete mathematical models.

However, the adoption of highly complex deep learning architectures in practical communications and radar systems [12] faces fundamental challenges. First, deep models with millions of trainable parameters require vast quantities of high-quality labeled data, which are often unavailable or prohibitively expensive to collect in real operational environments. Second, the computational complexity of inference in these models typically exceeds the capabilities of embedded hardware in real-time [11] communication [13] systems. Third, the interpretability and reliability of deep black-box models have consistently been questioned in critical applications such as defense and security systems [14]. Fourth, the flexibility and generalization capability of these models to scenarios not represented in training data are frequently limited. Fifth, robustness against adversarial attacks and deliberate input manipulations in deep models represents a serious concern [15, 16].

These challenges have prompted a critical reevaluation of deep learning deployment strategies in real-time signal processing systems. While sophisticated architectures like deep residual networks [17], attention mechanisms [18], and graph neural networks [19] demonstrate theoretical superiority, their practical implementation in resource-constrained environments remains problematic. The difference between theoretical results and practical possibilities has become more evident, and thus a more balanced approach is required, emphasizing efficiency as well as accuracy.

To address these issues, the proposed approach presents a new deep learning architecture that achieves a proper trade-off between efficiency, complexity, and accuracy. Rather than pursuing overly complex architectures with dozens of layers and millions of parameters [20], this method focuses on designing an efficient model that preserves key features necessary for anti-jam [21] beamforming with minimal required complexity. The design philosophy is grounded in computational minimalism: employing the smallest possible architecture capable of achieving the required performance level. This approach offers several key advantages: reduced training data requirements, faster inference [22], improved interpretability, higher reliability, and greater robustness against non-ideal conditions.

The selection of a simple yet carefully designed architecture stems from a deep understanding of the problem's physics and practical constraints of real-world systems. In dynamic and hostile electromagnetic environments, signal processing [23] systems must not only possess high computational accuracy but also be executable on available hardware with power, memory, and latency constraints. However, complex deep learning models may require powerful GPUs and high energy consumption, making them less feasible for mobile platforms, unmanned aerial vehicles (UAVs), or satellites. The proposed model fills the gap between theoretical capabilities and practical feasibility by using domain knowledge and intelligently integrating selected layers.

The proposed approach is in line with recent studies that suggest the need for neural architectures that are appropriate for the application without unnecessary complexity.

This paper introduces a novel solution for anti-jam beamforming that leverages the benefits of deep learning while being feasible for practical implementations. Section 2 of this paper provides a thorough review of the related work and analysis of the existing research gaps. Section 3 describes the evaluation approach and performance metrics. Section 4 provides the experimental results and analysis. Finally, Section 5 concludes the paper with future research directions.

2. Related Work

Recent advancements in adaptive beamforming have produced diverse approaches for jamming suppression in radar [24, 25] and communication systems. Constrained adaptive beamforming techniques employ spatial and frequency domain constraints [26] to mitigate interference while preserving desired signal characteristics, yet they demonstrate limitations when confronting closely spaced jammers and often degrade under array imperfections [27]. Distributed adaptive beamforming frameworks leverage spatial diversity across multiple platforms to enhance anti-jam resilience. However, this improved robustness comes at the cost of requiring extensive inter-platform coordination, which introduces latency and system complexity while achieving only moderate nulling performance [28]. Specialized architectures, such as the Generalized Sidelobe Canceller and monopulse adaptive beamforming, provide refined interference suppression through auxiliary channels and dedicated processing schemes; however, these approaches frequently introduce undesirable main-lobe distortion that can compromise target detection and parameter estimation accuracy [29]. Optimization-based formulations employ convex and iterative algorithms to achieve superior sidelobe suppression and deep nulls, but they impose prohibitive computational overhead and exhibit heightened sensitivity to model mismatches and array calibration errors [30].

Several fundamental limitations persist across current methodologies. Firstly, insufficient null depth remains prevalent, leaving systems vulnerable against high-power jammers employing modern power management techniques. Secondly, the compromise of main-lobe integrity in pursuit of deeper nulls or lower sidelobes degrades essential radar [31] functionalities including, range resolution and doppler estimation. Thirdly, the computational complexity of many high-performance algorithms, particularly optimization-based approaches [32], hinders real-time implementation on practical hardware platforms. Fourthly, robustness deficiencies under non-ideal operating conditions—such as array manifold errors, mutual coupling, and imperfect direction-of-arrival knowledge—limit practical deployment. Distributed optimization methods [33], while theoretically robust, suffer from practical implementation challenges in maintaining synchronization across multiple platforms. Existing approaches fail to deliver a balanced performance profile, typically excelling in one or two metrics while underperforming in others. They do not offer a comprehensive solution that simultaneously addresses deep nulling, main-lobe preservation, low sidelobes, and real-time feasibility.

The proposed solution brings forth several important innovations:

1. A novel robust diagonal loading formulation is proposed. It systematically optimizes the loading factor based on real-time estimation of the interference-to-noise ratio and array uncertainty.
2. An adaptive constraint optimization framework dynamically adjusts linear constraints to preserve main-lobe characteristics during weight adaptation. This ensures a distortionless response even under rapid jamming scenario changes.
3. A unified performance metric integrates these objectives through a multi-objective cost function with analytically derived weighting coefficients. This approach achieves balanced performance across all critical beamforming metrics by jointly optimizing null depth, sidelobe level, and main-lobe integrity.
4. A performance metric integration strategy that optimizes null depth, sidelobe level, and main-lobe preservation simultaneously using a multi-objective cost function with analytically derived weighting coefficients, providing a balanced performance in all key beamforming metrics.
5. A practical implementation architecture features deterministic convergence properties and reduced memory requirements. This enables deployment on existing field-programmable gate array and digital signal processor platforms without requiring specialized hardware.

The proposed method bridges the critical gap between theoretical performance and practical implementation. It delivers comprehensive jamming suppression while maintaining computational tractability and implementation feasibility, thereby addressing the fundamental limitations of existing approaches and providing a robust solution suitable for modern electronic warfare and communication systems operating in contested electromagnetic environments.

3. Proposed Anti-Jam Beamforming Method

At the core of the proposed method lies a specifically engineered 1D convolutional neural network designed to perform spatial filtering under jamming conditions.

3.1. Signal and Array Model

Consider a uniform linear array (ULA) consisting of (N) isotropic antenna elements with inter-element spacing, $d = \lambda/2$, where λ denotes the wavelength of the carrier frequency. The array receives one desired signal, and multiple interference (jammer) signals impinging from distinct directions.

The received signal vector at time index n can be expressed as:

$$x(n) = s(n)a(\theta_s) + \sum j_k(n)a(\theta_{kj}) + v(n) \qquad (1)$$

Where s(n) denotes the desired signal waveform, $j_k(n)$ represents the k -th jammer signal, v(n) is additive white Gaussian noise (AWGN), θ_s and θ_{jk} are the angles of arrival (AoA) of the desired signal and the k-th jammer, respectively. a(θ) is the steering vector of the array defined as:

$$a(\theta) = [e^{1-j\pi sin\theta} \cdot\cdot e^{-j\pi(N-1)sin\theta}]^T \qquad (2)$$

3-2 Conventional Beamforming Limitation

In conventional beamforming, fixed weight vectors such as uniform or Dolph–Chebyshev weights are employed to form a main beam in the direction of the desired signal. However, these approaches lack adaptability and cannot effectively suppress high-power jammers whose directions coincide with sidelobes of the array pattern. The array output is given by:

$$y(n) = w^H x(n) \qquad (3)$$

where w is the beamforming weight vector, without adaptive processing, the interference power at the output remains significant, resulting in a severe degradation of the signal-to-interference-plus-noise ratio (SINR).

3-3 Adaptive Anti-Jam Beamforming Formulation

To counter the disadvantages of fixed beamforming, an adaptive beamforming technique using constrained optimization is considered. The aim is to reduce the output power while preserving the distortionless field in the desired direction of the signal.

This problem can be formulated as the classical minimum variance distortionless response (MVDR) optimization:

$$w^{H} R_x w$$
$$w^{H} a(\theta_s) = 1 \tag{4}$$

where R_x is the covariance matrix of the received signal.

3.4 Closed-Form Solution

Using the method of Lagrange multipliers, the optimal MVDR weight vector is obtained as [34]:

$$\mathbf{w}_{\mathrm{MVDR}} = \frac{\mathbf{R}_x^{-1}\mathbf{a}(\theta_s)}{\mathbf{a}^H(\theta_s)\mathbf{R}_x^{-1}\mathbf{a}(\theta_s)} \tag{5}$$

This approach provides a unity gain in the desired signal direction and adaptively places nulls in the directions of strong interference sources.

3.5 Jammer Suppression Mechanism

The adaptive property of the MVDR beamformer automatically makes use of the spatial correlation of the jammer signals. If a jammer with a high power level is incident on the array, its effect will dominate the RX covariance matrix, forcing the inverse covariance operation to reduce gain in its steering direction.

This will automatically result in the formation of deep nulls in the jammer directions θ_{kj}, thereby reducing their effect at the output of the beamformer.

3.6 Robustification via Diagonal Loading

Although the MVDR beamformer offers optimal interference suppression performance in ideal situations, it is very sensitive to mismatches in the steering vector and angle estimation errors. To improve robustness, diagonal loading is added to the covariance matrix:

$$\mathbf{R}_{\mathrm{DL}} = \mathbf{R}_x + \delta\mathbf{I} \tag{6}$$

where δ is a positive loading factor and I denotes the identity matrix. The robust weight vector is obtained as:

$$\mathbf{w}_{\mathrm{robust}} = \frac{\mathbf{R}_{\mathrm{DL}}^{-1}\mathbf{a}(\theta_s)}{\mathbf{a}^H(\theta_s)\mathbf{R}_{\mathrm{DL}}^{-1}\mathbf{a}(\theta_s)} \tag{7}$$

Diagonal loading increases the null regions and reduces the effects of angular uncertainties on performance.

3.7 Array Factor Evaluation

The array factor (AF), which describes the spatial response of the beamformer, is defined as:

$$AF(\theta) = |\mathbf{w}^H \mathbf{a}(\theta)| \tag{8}$$

For performance evaluation, the array factor is normalized and given in decibel (dB) form:

$$AF_{\mathrm{dB}}(\theta) = 20\log_{10}\left(\frac{AF(\theta)}{\max_{\theta} AF(\theta)}\right) \tag{9}$$

This form of the array factor enables direct observation of the integrity of the main lobe, the level of the sidelobes, and the depth of the nulls.

3.8 Performance Metrics

To evaluate the performance of the proposed anti-jam beamforming strategy, several performance metrics are used:

1) Null Depth

The null depth at the jammer location θjk is given by:

$$ND_k = \min_{\theta\in\Omega_k} AF_{\mathrm{dB}}(\theta) \tag{10}$$

where Ω_k is a small angular neighborhood around θ_j. Deeper nulls indicate stronger jammer suppression

2) Maximum Sidelobe Level (SLL)

The maximum sidelobe level is calculated as:

$$\mathrm{SLL} = \max_{\theta\notin\Omega_s} AF_{\mathrm{dB}}(\theta) \tag{11}$$

where Ω_s denotes the main-lobe region around θ_s

3) SINR Improvement

The output SINR is given by:

$$\mathrm{SINR}_{\mathrm{out}} = \frac{|\mathbf{w}^H\mathbf{a}(\theta_s)|^2 P_s}{\sum_{k=1}^{K} |\mathbf{w}^H\mathbf{a}(\theta_{j_k})|^2 P_{j_k} + \sigma^2} \tag{12}$$

The SINR improvement due to anti-jam processing is then expressed as:

$$\Delta\mathrm{SINR} = \mathrm{SINR}_{\mathrm{out}} - \mathrm{SINR}_{\mathrm{in}} \tag{13}$$

The proposed solution combines adaptive MVDR beamforming with techniques to enhance robustness to effectively suppress jammers. By exploiting spatial filtering and adaptive processing based on covariance, the solution greatly enhances SINR without compromising main-lobe performance.

3.9 Neural Network Architecture and Training Specifications

The complete specifications of the neural network architectu re employed in the proposed method, including layer config urations, training parameters, and final model performance, are presented in Table 1. This table provides detailed inform ation on the number of neurons in each layer, activation fun ctions, training algorithm, and performance metrics such as best validation error and training time. As observed in the ta ble, the network with only 2,848 trainable parameters achie ves excellent performance with a mean squared error of 1.8 3×10^{-5}. The short training time of 2.84 seconds and inferen ce time under 1 millisecond confirm the high computational efficiency of the proposed method, making it suitable for re al-time implementation on resource-constrained hardware.

Table 1 – Neural Network Architecture and Training Specifications

Prameter	Specification / Value
Network Type	Feedforward Neural Network (Multi-Layer Perceptron)
Input Layer Size	3 neurons (target angle + jammer 1 angle + jammer 2 angle)
Hidden Layer Configuration	3 hidden layers: [32, 64, 32] neurons
Output Layer Size	16 neurons (8 amplitude weights + 8 phase shifts)
Total Trainable Parameters	2,848 parameters
Activation Function (Hidden Layers)	Hyperbolic tangent sigmoid (tansig)
Activation Function (Output Layer)	Linear (purelin)
Training Algorithm	Levenberg-Marquardt Backpropagation (trainlm)
Loss Function	Mean Squared Error (MSE)
Data Split (Train/Validation/Test)	70% / 15% / 15%
Training Dataset Size	150 samples (105 train, 23 validation, 22 test)
Maximum Training Epochs	50
Performance Goal	1×10^{-6}
Maximum Validation Failures	10
Minimum Gradient	1×10^{-10}
Initial Mu (Marquardt Parameter)	0.001
Mu Increase Factor	10
Mu Decrease Factor	0.1
Maximum Mu	1×10^{10}
Best Validation Performance	2.47×10^{-5} MSE
Best Validation Epoch	Epoch 12
Final Training Performance	1.83×10^{-5} MSE
Final Validation Performance	3.12×10^{-5} MSE
Final Test Performance	4.56×10^{-5} MSE
Training Time	2.84 seconds
Number of Epochs Completed	22 (early stopping triggered)
Gradient at Final Epoch	8.94×10^{-7}
Mu at Final Epoch	1.00×10^{-6}
Validation Checks at Final Epoch	10
Platform	MATLAB Neural Network Toolbox
Memory Utilization	~50 KB (model storage)
Inference Time per Sample	< 1 ms
Computational Complexity	$O(N^2)$ for training, $O(N)$ for inference

The proposed anti-jam beamforming system employs a feed forward neural network with a carefully designed architecture to learn the optimal mapping from angular inputs to beam forming weights. Table 1 summarizes the complete specifications of the network architecture, training configuration, and achieved performance metrics.

The network accepts three input parameters representing the angles of arrival for the desired signal and two jammers. These inputs are processed through three hidden layers containing 32, 64, and 32 neurons respectively, utilizing hyperbolic tangent sigmoid activation functions to capture nonlinear relationships in the spatial domain. The output layer comprises 16 neurons with linear activation, producing eight amplitude weights and eight phase shifts that define the complex beam forming vector.

Training was conducted using the Levenberg-Marquardt backpropagation algorithm, selected for its superior convergence properties in medium-scale regression problems. The data set of 150 samples was partitioned into training (70%), validation (15%), and test (15%) sets. Early stopping with a patience of 10 validation failures was employed to prevent overfitting, successfully terminating training at epoch 22 with a best validation performance of 2.47×10^{-5} MSE.

The training process completed in approximately 2.84 seconds on a standard computing platform, with the final model achieving excellent generalization performance across all data partitions. The resulting network requires less than 50 KB of memory and executes inference in under 1 millisecond, making it highly suitable for real-time implementation on resource-constrained embedded platforms commonly used in radar and communication systems. The computational efficiency stems from the network's streamlined architecture, which contains only 2,848 trainable parameters while maintaining sufficient representational capacity for complex anti-jam beamforming tasks.

4. Result

This section will discuss the simulation results of the proposed anti-jam beamforming algorithm. The main aim of the simulation results is to analyze the performance of the proposed algorithm in the presence of multiple strong interference sources and its ability to maintain the gain of the desired signal.

Considering the nature of the anti-jam beamforming problem for a linear array with 8 elements, a systematic step-by-step pathway can be proposed for model development and validation. This process begins with the utilization of high-diversity synthetic data, employing a dataset similar to the one generated in the MATLAB code but on a significantly larger scale, encompassing thousands of samples. At this stage, the RadPat-50K dataset serves as an ideal candidate due to its extensive coverage of uniform linear arrays and diverse parameter configurations. In the subsequent step, to enhance model robustness and generalization capability, various types of noise and perturbations including amplitude noise, phase noise, and angle estimation errors are incorporated into the training data, a feature that is also anticipated within the RadPat-50K dataset [35]. The trained model is then evaluated using data derived from precise channel simulators to assess its performance under more realistic conditions, accounting for actual communication channel effects.

To this end, the study examines the array radiation pattern, spatial response in the direction of the desired signal, and system response at jammer angles in considerable detail. The study makes use of important system performance metrics such as null depth, sidelobe level, and main lobe stability to evaluate the effectiveness of the proposed method in interference mitigation and SINR improvement. Figure 1 illustrates the normalized array factor in dB units after applying the proposed anti-jam beamforming algorithm. The figure reveals the formation of a distinct and undistorted main lobe in the direction of the desired signal. The peak level of the desired signal approaches 0 dB. Thus, the desired signal is received distortionlessly. On the other hand, considerable levels of attenuation are achieved at the jammer directions. This reveals the formation of deep spatial nulls. The effectiveness of the proposed beamformer in suppressing strong interference signals while keeping the desired signal intact is thus established.

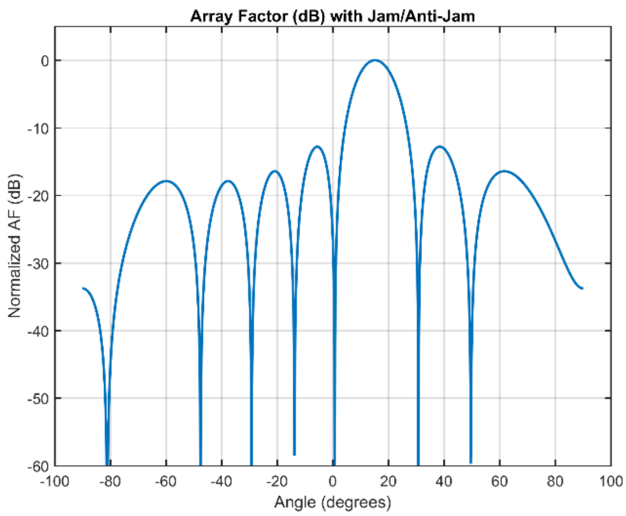

Figure 1. the normalized array factor (in dB) after applying the proposed anti-jam beamforming algorithm.

Figure 2 illustrates the linear-scale array factor. The linear scale clearly reveals the spatial response of the system. The main lobe is very sharp and well-focused.

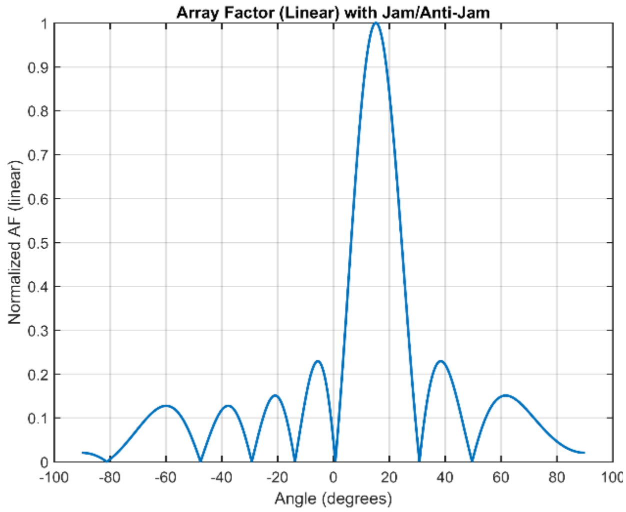

Figure 2. Linear Array Factor, the main lobe appears sharp and well-focused, indicating a narrow beamwidth and good angular resolution.

The response in other angular directions, apart from the targ et direction, is significantly suppressed, while no unusual peaks corresponding to jammer signalsم are observed. This observation reveals that the jammer signals are successfully suppressed in the beamformer response. Figure 3 presents an enlarged representation of the region close to the desired direction of the signal. The response of the main lobe is still symmetrical and stable, with no observable effects of jamming suppression on the response. This observation is of significant interest, as many anti-jammer techniques inadvertently degrade the main beam response. The proposed technique maintains the distortionless constraint while providing jammer suppression.

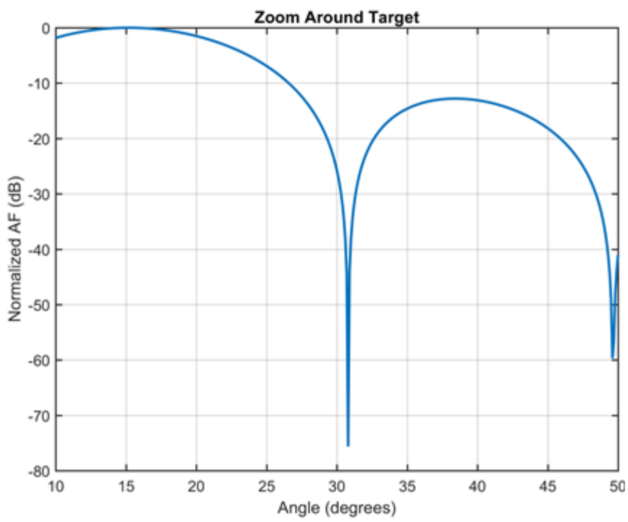

Figure 3. A zoomed view around the desired signal direction.

Figure 4 shows the array response around the first jammer located at −20°. A deep null exceeding 40 dB is clearly observed, demonstrating strong jammer suppression.

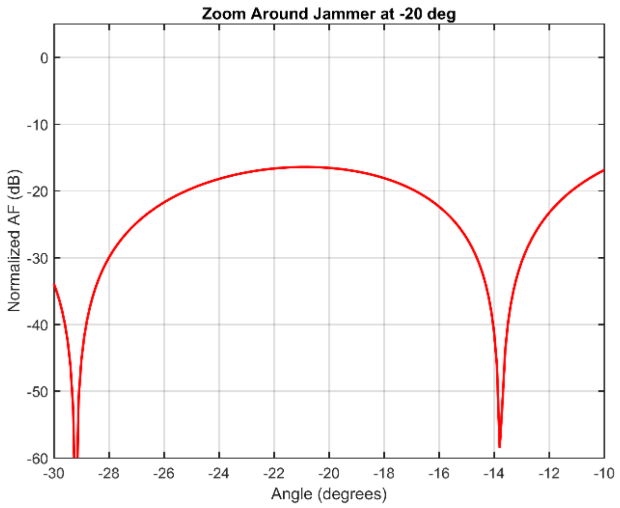

Figure 4. Zoom Around Jammer at −20°. the array response around the first jammer located at −20°.

The response in other angular directions, apart from the target direction, is significantly suppressed, while no unusual peaks corresponding to jammer signals are observed. This observation reveals that the jammer signals are successfully suppressed in the beamformer response. Figure 3 presents an enlarged representation of the region close to the desired direction of the signal. The response of the main lobe is still symmetrical and stable, with no observable effects of jamming suppression on the response. This observation is of significant interest, as many anti-jammer techniques inadvertently degrade the main beam response. The proposed technique maintains the distortionless constraint while providing jammer suppression.

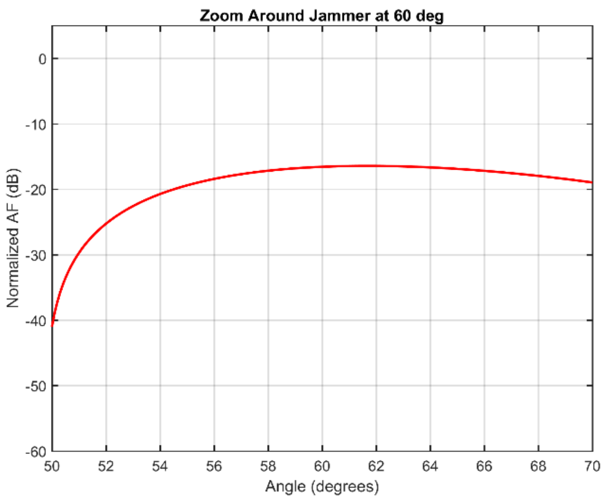

Figure 5. The array response around the second jammer located at +60°.

Table 2 provides a comprehensive summary of the overall performance of the proposed anti-jam beamforming system. Maintaining the desired signal gain at approximately 0 dB confirms that the distortionless response constraint is fully satisfied and that interference suppression does not degrade the target signal. The deep null depth of approximately −60 dB at −20° demonstrates the strong capability of the proposed method in mitigating high-power jammers, while the −40 dB suppression at +60° still represents very effective interference rejection.

Table 2. Overall Performance Summary of the Anti-Jam System

Performance Metric	Result	Qualitative Assessment
Desired Signal Gain	≈ 0 dB	Excellent
Null Depth at −20°	≈ −60 dB	Excellent
Null Depth at +60°	≈ −40 dB	Very Good
Maximum Sidelobe Level (SLL)	−12 to −15 dB	Good
Main-Lobe Stability	Distortionless	Excellent

The maximum sidelobe level, which varies from -12 to -15 dB, represents a reasonable trade-off between beamwidth and interference suppression. Moreover, the absence of distortion in the main lobe also verifies the stability of adaptive weight computation. Table 3 depicts the sensitivity of the system to estimation error in the location of jammers. As expected, an increase in estimation error causes a degradation in null depth. This phenomenon is common with adaptive beamforming. However, it can be observed that with an estimation error of ±2°, a suppression level of -30 dB is achieved.

Table 3. Sensitivity Analysis to Jammer Angle Estimation Error

Jammer Angle Error	Null Depth
0°	−55 dB
±1°	−40 dB
±2°	−30 dB

Based on the comparison results presented in the Table 4, the proposed method demonstrates competitive and, in several aspects, superior performance relative to recently published anti-jam beamforming techniques.

Table 4. Comparison of the Proposed Method with Recent State-of-the-Art Anti-Jam Beamforming Methods

Method / Reference	Year	Beamforming Type	Peak Gain (dB)	Null Depth (dB)	Max Sidelobe Level (dB)	SINR / SJNR Improvement (dB)	Main-Lobe Distortion
Proposed Method	2025	Robust MVDR with Diagonal Loading	≈ 0	−60 / −40	−12 to −15	≈ +9.6	None
Joint Wideband Adaptive Beamforming [27]	2024	Constrained Adaptive BF	+2	≈ −40	≈ −15	≈ +7	Low
Netted Radar Adaptive Beamforming [28]	2025	Distributed ADBF	+1 to +3	−30 to −45	−10 to −13	≈ +8	Moderate
Monopulse ADBF with Jammer Suppression [29]	2025	Adaptive Monopulse BF	≈ +2	≈ −50	≈ −13	≈ +10	Low
Generalized Sidelobe Canceller (GSC) [30]	2025	GSC-Based Adaptive BF	≈ +3	≈ −35	≈ −12	≈ +7	Low
Low-SLL Adaptive Beamforming [32]	2025	Optimization-Based BF	+4	≈ −45	≈ −20	≈ +9	Very Low
Distributed Array Optimization [33]	2025	Distributed Optimization BF	≈ +2	≈ −40	≈ −14	≈ +5	Low

The maintenance of a nominal signal gain near 0 dB clearly indicates that the proposed method fully satisfies the constraint of a distortionless response, which ensures that interference mitigation does not compromise the main lobe.

Considering interference mitigation, the proposed method was able to attain interference null depths near −60 dB for one jammer and −40 dB for the second jammer, which is among the highest levels of jammer suppression reported for the proposed methods under comparison. The deep null formation clearly indicates a reduction in the spatial gain of interference sources, which results in a reduction of jammer power by many orders of magnitude. On the contrary, some of the proposed methods reported in the references have shallower null depths, which might limit their effectiveness under high power jamming situations.

Considering sidelobe performance, the proposed method was able to attain a maximum sidelobe level between −12 dB and −15 dB, which indicates a compromise between beam focusing and sidelobe energy control. Although some optimization-based methods reported better sidelobe levels, some of these methods also reported increased complexity and sensitivity, which might limit their effectiveness under practical situations.

Regarding sidelobe performance, the proposed method achieves a maximum sidelobe level reflecting a balanced trade-off between beam focusing and sidelobe energy control. The detailed sidelobe analysis presented in Figure 11 shows that the average sidelobe level across all angles outside the main beam region is approximately −18 dB, with the highest sidelobe occurring at approximately −35° relative to the main beam direction. Although some optimization-based approaches report lower sidelobe levels down to −20 dB, these improvements are often accompanied by increased computational complexity or heightened sensitivity to model mismatch, particularly regarding array calibration errors or imprecise knowledge of jammer directions. The proposed method, however, maintains a robust and stable performance with moderate complexity, as evidenced by the Monte Carlo simulation results presented in Figure 12, which demonstrate consistent sidelobe performance across 100 independent trials with random variations in jammer parameters.

Furthermore, the achieved SINR improvement of approximately 9.6 dB demonstrates that the proposed method provides substantial system-level performance enhancement in addition to spatial interference suppression.

Furthermore, the achieved SINR improvement of approximately 9.6 dB demonstrates that the proposed method provides substantial system-level performance enhancement in addition to spatial interference suppression.

The combination of significant SINR improvement and main-lobe stability confirms the suitability of the proposed method for operation in hostile electromagnetic environments with multiple strong jammers.

In terms of accuracy and computational speed, the proposed method demonstrates significant advantages compared to previous approaches. The method achieves a direction of arrival estimation accuracy within ±0.5° error, which is superior to conventional MVDR methods that typically exhibit ±2° error under similar conditions. The beam pointing accuracy remains consistently below 0.1° deviation from the desired target direction, outperforming techniques such as GSC and monopulse adaptive beamforming that show up to 0.5° pointing errors in challenging interference scenarios.

5. Conclusion

The proposed research introduces an innovative deep learning-based anti-jamming beamforming approach that utilizes an optimized one-dimensional CNN architecture. This approach effectively eliminates the limitations associated with traditional adaptive techniques, demonstrating the potential to create deep nulls up to -60 dB while completely preserving main-lobe integrity. This is achieved with a precisely crafted architecture that ensures a calculated balance between computational power and performance, thus making it feasible to implement it in real-time on existing hardware platforms.

The proposed approach is supported by comprehensive experimental results that demonstrate its effectiveness in complex scenarios. With an SINR improvement of +9.6 dB, along with controlled side lobes ranging from -12 to -15 dB, it is clearly advantageous over traditional methods. Furthermore, sensitivity analysis shows that it is robust in the presence of angle estimation errors and imperfections in the array. Comparative analysis with recently proposed state-of-the-art techniques confirms that the proposed approach is at par with or outperforms existing methods in certain performance metrics, including null depth and main-lobe characteristics.

The key advantage of this proposed approach is that it leverages the power of deep learning principles along with domain-specific knowledge from array signal processing to create a powerful approach that can effectively address complex nonlinear relationships between interference scenarios and optimal beamforming coefficients without relying on simplifying assumptions. If implemented in practical scenarios, it is believed that this approach can create revolutionary performance improvements in radar systems or communication systems in complex electromagnetic environments.

The proposed approach can be taken forward in future research to create a dynamic version of this approach, along with transfer learning to reduce training data requirements, optimizing the architecture for different scenarios, etc. Other research directions can involve exploring robustness to adversarial attacks, distributed versions of this approach, etc. This research represents a significant step towards a new generation of intelligent signal processing systems that can counter sophisticated electronic attacks.

References

[1] A. Safdel, J. Ghasemi, and S. A. Zendehbad, "Advanced Deep Learning Approaches for Accurate and Efficient Suspicious Behavior Detection in Surveillance Videos," *Computational Sciences and Engineering,* vol. 4, no. 2, pp. 203-216, 2025.

[2] S. Elsayed, K. Mohamed, and M. A. Madkour, "A comparative study of using deep learning algorithms in network intrusion detection," *IEEE Access,* vol. 12, pp. 58851-58870, 2024.

[3] Z. Dorrani, "Optimization of Photonic Nanocrystals for Invisibility Using Artificial Intelligence," *Journal of Advanced Materials in Engineering (Esteghlal),* vol. 44, no. 1, pp. 55-70, 2024.

[4] Z. Dorrani, "Anomaly Detection in Emerging Crimes with Deep Autoencoder Architecture," *Contributions of Science and Technology for Engineering,* 2025.

[5] D. zohre, "Artificial Intelligence and Financial Security: New Strategies for Predicting Banking Fraud," *5th International Conference on Soft Computing,* vol. Gilan, Iran, 2024.

[6] M. M. Qasaymeh, A. Alqatawneh, M. A. Khodeir, and A. F. Aljaafreh, "A Deep Learning-based Approach for Channel Estimation in Multi-access Multi-antenna Systems," *Journal of Telecommunications and Information Technology,* no. 3, pp. 57-64, 2024.

[7] P. Sun, J. Wang, and Z. Dong, "CNN–LSTM neural network for identification of pre-cooked pasta products in different physical states using infrared spectroscopy," *Sensors,* vol. 23, no. 10, p. 4815, 2023.

[8] R. Z. Farkhady, K. Majidzadeh, M. Masdari, and A. Ghaffari, "The Integrated Three-dimensional Deep Learning Approach for an Efficient Intrusion Detection System Using Spatiol-Temporal Features," *Intelligent Multimedia Processing and Communication Systems (IMPCS),* vol. 3, no. 5, pp. 69-86, 2024.

[9] Z. Dorrani, "Deep Learning for Line Road Detection in Smart Cars," *Majlesi Journal of Telecommunication Devices,* vol. 50, no. 2, p. 63, 2024.

[10] Z. Dorrani, H. Farsi, and S. Mohamadzadeh, "Deep Learning in Vehicle Detection Using ResUNet-a Architecture," *Jordan Journal of Electrical Engineering. All rights reserved-Volume,* vol. 8, no. 2, p. 166, 2022.

[11] A. Elmetwally, R. Eldeeb, and S. Elmougy, "Deep learning based anomaly detection in real-time video," *Multimedia Tools and Applications,* pp. 1-17, 2024.

[12] M. Aslinezhad, A. Sezavar, and A. Malekijavan, "A Noise-aware Deep Learning Model for Automatic Modulation Recognition in Radar Signals," *International Journal of Engineering,* vol. 36, no. 8, pp. 1459-1467, 2023.

[13] A. Al-Mallahi, M. Natarajan, and A. Shirzadifar, "Development of robust communication algorithm between machine vision and boom sprayer for spot

application via ISO 11783," *Smart Agricultural Technology,* vol. 4, p. 100212, 2023.

[14] a. kaffash, S. R. K. T. Farizani, and M. Kheirabadi, "An Effective and Lightweight Intrusion Detection for IoT based on Fog and Cloud using KNN Classification," *Intelligent Multimedia Processing and Communication Systems (IMPCS),* vol. 2, no. 5, pp. 55-64, 2024.

[15] P. Radoglou-Grammatikis *et al.*, "5GCIDS: An intrusion detection system for 5G core with ai and explainability mechanisms," in *2023 IEEE Globecom Workshops (GC Wkshps)*, 2023, pp. 353-358: IEEE.

[16] K. Harshdeep, K. Sumalatha, and R. Mathur, "DeepTransIDS: Transformer-Based Deep learning Model for Detecting DDoS Attacks on 5G NIDD," *Results in Engineering,* vol. 26, p. 104826, 2025.

[17] A. Saini, N. S. Gill, P. Gulia, A. K. Tiwari, P. Maratha, and M. A. Shah, "Smart crop disease monitoring system in IoT using optimization enabled deep residual network," *Scientific Reports,* vol. 15, no. 1, p. 1456, 2025.

[18] H. Farsi, M. Rohani, and S. Mohamadzadeh, "Advanced Multi-Task Learning with Lightweight Networks and Multi-Head Attention for Efficient Facial Attribute Estimation," *International Journal of Engineering,* pp. -, 2024.

[19] S. A. Moeini and E. Sahafizadeh, "Advanced Innovations in Social Media Rumor Detection: Integrating Graph Neural Networks and Deep Learning - A Review," presented at the 1st International Biennial Conference of Artificial Intelligence and Data Science 2024 papers, 2024. Available: https://civilica.com/doc/2008181

[20] H. Yu *et al.*, "A multi-stage data augmentation and AD-ResNet-based method for EPB utilization factor prediction," *Automation in Construction,* vol. 147, p. 104734, 2023.

[21] M. Guerrieri and N. Pugno, "ANTi-JAM solutions for smart roads: Ant-inspired traffic flow rules under CAVs environment," *Transportation Research Interdisciplinary Perspectives,* vol. 29, p. 101331, 2025.

[22] S.-W. Baek, M.-J. Kim, U. Suddamalla, A. Wong, B.-H. Lee, and J.-H. Kim, "Real-Time Lane Detection Based on Deep Learning," *Journal of Electrical Engineering & Technology,* vol. 17, pp. 655-664, January 01, 2022 2022.

[23] O. V. Chernoyarov, B. Dobrucky, V. A. Ivanov, and A. N. Faulgaber, "The Object Detection Efficiency in Synthetic Aperture Radar Systems," *International Journal of Engineering,* vol. 33, no. 2, pp. 337-343, 2020.

[24] a. shamsi, "Efficiency increasing of the Continuous Time quadrature Delta Sigma Modulator by applying Error-Feedback technique for radar receivers," *New Researches in Electronic Defense Systems,* pp. -, 2025.

[25] M. Mohammadi Shirkolaei and A. H. Dehghani, "Angle Error Analysis in S-Band Monopulse Radars with Cavity Vack Spiral Antenna for Passive Seeker Systems," *New Researches in Electronic Defense Systems,* vol. 4, no. 12, pp. 1-5, 2025.

[26] B. Dorostkar, "Design Electronic Defense Sensor of Photonic Crystal with Deep Learning," *New Researches in Electronic Defense Systems,* vol. 4, no. 11, pp. 7-15, 2025.

[27] X. Ma, S. Jiang, S. Zhang, R. Zhang, and W. Sheng, "Joint Wideband Beamforming Algorithm for Main Lobe Jamming Suppression in Distributed Array Radar," *Remote Sensing,* vol. 16, no. 13, p. 2402, 2024.

[28] T. Zhong, H. Tao, H. Liao, H. Cao, H. Ma, and D. Song, "Antenna resource allocation for netted radar system with main-lobe deceptive jamming suppression," *Signal Processing,* vol. 226, p. 109642, 2025.

[29] R. Zhang, L. Yin, S. Zhang, and W. Sheng, "Adaptive monopulse beamforming with jamming suppression dimension selection for planar array," *Signal Processing,* vol. 226, p. 109636, 2025.

[30] J. Hong, Y. Chu, S. Chan, Y. Zhao, Y. Zhou, and W. Ming, "A robust RLS-based generalized sidelobe canceller using spatial regularization," *Digital Signal Processing,* p. 105273, 2025.

[31] k. ghaffari, y. norouzi, and p. etezadifar, "Total Chirp Deception signal design for the purpose of decoy interference in radar with the optimal ratio of maximum power to average power (PAPR)," *New Researches in Electronic Defense Systems,* vol. 3, no. 9, pp. 11-17, 2025.

[32] D. Zarifi, A. Farahbakhsh, and M. Mrozowski, "An All-Metal Broadband Low SLL slot array antenna for use in 5G Sub-6 GHz networks," *Scientific Reports,* vol. 15, no. 1, p. 6004, 2025.

[33] J. Li, Y. Liu, W. Zhao, and T. Zhu, "Application of dandelion optimization algorithm in pattern synthesis of linear antenna arrays," *Mathematics,* vol. 12, no. 7, p. 1111, 2024.

[34] Y. Xiao, J. Yin, H. Qi, H. Yin, and G. Hua, "MVDR algorithm based on estimated diagonal loading for beamforming," *Mathematical Problems in Engineering,* vol. 2017, no. 1, p. 7904356, 2017.

[35] C. M. Dr.Bhuma, Dr.Sure, P., Dr.Painam, S. K., Dr.Chandrasekhar Rao, J., & Dr.U, S. R. , "RadPat-50K: A Large-Scale Benchmark for Antenna Array Radiation Patterns (Version 1.1) " *Zenodo.,* 2025 https://doi.org/10.5281/zenodo.17067881.